

Characterization of sol–gel derived $\text{Pb}(\text{Zr}_{0.3}\text{Ti}_{0.7})\text{O}_3/\text{PbTiO}_3$ multilayer thin films

Lingling Sun, Ooi Kiang Tan*, Weiguo Liu, Weiguang Zhu, Xiaofeng Chen

*Sensors and Actuators Laboratory, School of Electrical and Electronic Engineering,
Nanyang Technological University, Singapore 639798, Singapore*

Received 1 December 2003; received in revised form 9 December 2003; accepted 22 December 2003

Available online 30 April 2004

Abstract

Ferroelectric $\text{Pb}(\text{Zr}_{0.3}\text{Ti}_{0.7})\text{O}_3/\text{PbTiO}_3$ multilayer thin films are fabricated by the sol–gel method. The properties of PZT/PT multilayer thin films with different PZT and PT layers stacking structures have been systematically studied. All the films are dense and smooth with single perovskite phase. “Pinched” ferroelectric hysteresis loops are found for multilayer thin films. The dielectric constant of multilayer thin film decreases when the PT volume fraction increases. The dielectric loss of 5PZT/4PT multilayer thin film are comparable to that of pure PZT, however, all the other multilayer thin films show much higher dielectric loss. When compared to the pure PZT thin film, the 5PZT/4PT multilayer film has comparable pyroelectric coefficient, reduced dielectric constant and comparable dielectric loss. Therefore, the 5PZT/4PT thin film shows higher pyroelectric detectivity figure of merit and is a promising material structure for pyroelectric application.

© 2004 Elsevier Ltd and Techna Group S.r.l. All rights reserved.

Keywords: Multilayer thin film; Lead zirconate titanates; Sol–gel; Dielectrics

1. Introduction

Since the mid 1980s, the ferroelectric thin films based on $\text{Pb}(\text{Zr,Ti})\text{O}_3$ (PZT) have received considerable attention as they can be applied for various applications, such as ferroelectric memories [1], pyroelectric detectors [2,3], and piezoelectric microactuators [4]. Generally, the electrical properties of ferroelectric thin films are dependent on the micro-structured properties of the films such as phase structures developed during the heat treatment, orientations of crystalline phase and the interface structure formed in the film or between electrodes and the film. Many researchers have studied the relation of electric properties with structural properties. The effects of electrode materials [5], the influence of various buffer layers [6] and multiple coating of different kinds of perovskite dielectric thin films [7] were investigated for various applications. We have also reported on the good properties of sol–gel derived pure PZT thin film [8]. In this paper, we have investigated the properties of sol–gel derived PZT/PT multilayer thin films. The effect

of various PZT and PT stacking sequence has been systematically studied. The stacking structure has been optimized for pyroelectric application.

2. Experimental

The films were fabricated using sol–gel technique. Solid precursors of PZT and PT were initially prepared and then dissolved into 2-methoxyethanol to form the solution for spin-coating. Detailed solution preparation procedures were described elsewhere [8]. The thin films were deposited onto the Pt-coated silicon wafers using a spin coater operated at 3000 rpm for 30 seconds. After the spin-coating, each layer was baked at 420 °C for 2 min on a hotplate before the next layer was deposited. The thickness of each backed layer was around 50 nm measured using an elipsometer. The spin-coating were repeated to reach the desired thickness. Lastly, the films were annealed at 640 °C for 30 min in air. To form the multilayer structure, the PZT and PT layers were deposited in various sequences. The schematic structures of the four different multilayer samples are shown in Fig. 1.

* Corresponding author. Tel.: +65-6790-5411; fax: +65-6791-2687.
E-mail address: eoktan@ntu.edu.sg (O. Kiang Tan).

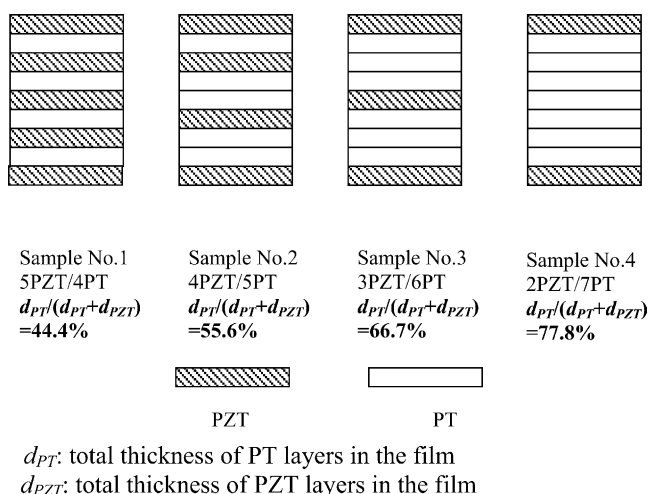


Fig. 1. Schematic structures of multilayer PZT/PT thin films.

The structural development of the ferroelectric films was investigated using the Shimadzu XRD-6000 X-ray diffractometer. The JEOL JSM-5310 scanning electron microscope (SEM) was used to observe the cross-section microstructure of the PZT thin films. For electrical measurement, platinum (100 nm) top electrodes of 0.1–0.2 mm² areas were sputtered through a shadow mask. The *I*–*V* behaviors of the thin films were investigated using a HP 4156 semiconductor parameter measurement unit. The characterization of dielectric constant and dielectric loss were carried out using the Solatron SI1260 impedance analyzer in conjunction with the SI1296 dielectric interface. The ferroelectric properties of the films were measured using the Precision Pro ferroelectric tester (Radiant Technologies, Inc.). The pyroelectric coefficients of the films were tested using the Byer–Roundy method.

3. Results and discussion

3.1. Microstructure of the thin films

Fig. 2 illustrates the XRD patterns of the multilayer thin films with different stacking structures. The peaks of multilayer thin films are believed to come from both the PZT and PT layers. However, the peaks from these two kinds of material layers are quite closed and cannot be set apart in our measurement. All thin films are composed of perovskite grains, and no pyrochlore phase can be detected within the detection limit of X-ray diffraction. Peak splitting such as (001)/{(100)(010)}, {(101)(011)}/(110) peak intensity doublet characteristics of the tetragonal structures are observed. It is observed that the $I_{(001)}/I_{\{(100)(010)\}}$ ratio becomes higher with more PT composition in the multilayer films. This means the PT-rich samples have higher c-domain content.

Fig. 3 shows a cross-sectional picture of the 5PZT/4PT thin film. The film looks dense and smooth. The other three films show similar cross-sectional structure.

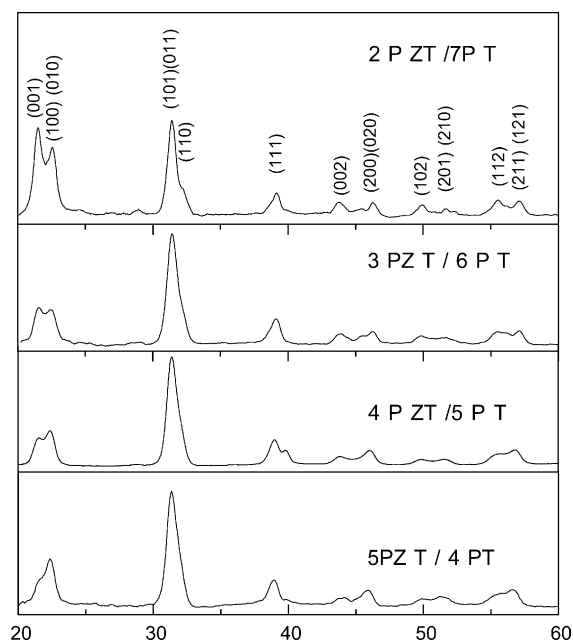


Fig. 2. XRD patterns of the multilayer PZT/PT thin films.

3.2. Dielectric properties

The *I*–*V* behaviors of the thin films are shown in Fig. 4. Pure PZT and pure PT thin films deposited using the same process are also characterized for comparison. Fig. 4 shows the pure PZT sample has a breakdown voltage around 23 V that is higher than that of pure PT's 16.5 V. All the four types of multilayer PZT/PT samples have lower breakdown voltage than the pure PZT and PT samples. This is because the PT layers have lower dielectric constant than PZT layers, when a voltage is applied on the films, most of the voltage will appear across the PT layers. As the PT layers have lower breakdown voltage than the PZT layers, and will breakdown earlier. Pure PZT and pure PT thin films show similar leakage current level. The multilayer 5PZT/4PT thin

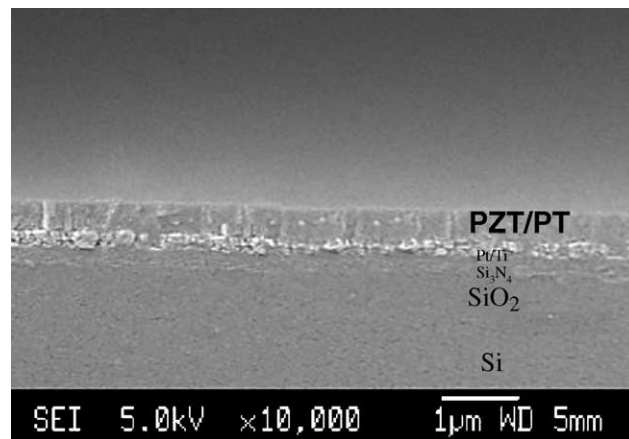


Fig. 3. SEM cross-section view of 5PZT/4PT thin film; the substrate is Pt (100 nm)/Ti (50 nm)/Si₃N₄ (200 nm)/SiO₂ (500 nm)/Si (450 μm).

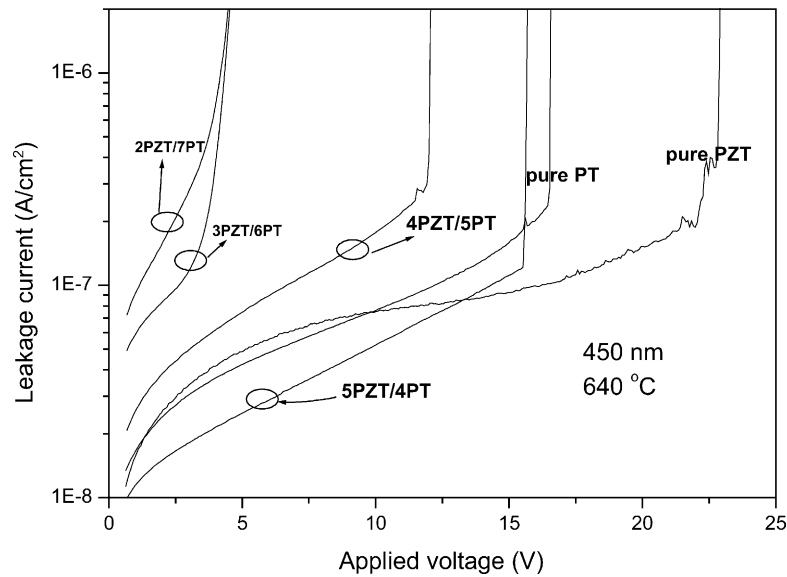


Fig. 4. Leakage current of the multilayer PZT/PT thin films.

film has a slightly lower leakage current when compared to those of pure PZT and pure PT samples. The other three types of multilayer samples show higher leakage current. It is suggested by J.J. Shyu and P.C. Lee that the PT layers of the thickness around 50 nm can effectively enhance the crystallinity and quality of the perovskite PZT layers, while a thicker PT interlayer do not have this enhancement property [9]. This may explain why the multilayer 5PZT/4PT film has relatively lower leakage current while all the other three types of multilayer samples have higher leakage current.

The PZT/PT multilayer capacitor can be considered as the PZT and PT capacitors connected in series. Therefore, the dielectric constant of the multilayer thin film can be

estimated using Eq. (1) as follows:

$$\varepsilon = \frac{\varepsilon_{PT}\varepsilon_{PZT}}{\varepsilon_{PT}V_{PZT} + \varepsilon_{PZT}V_{PT}} = \frac{\varepsilon_{PT}\varepsilon_{PZT}}{\varepsilon_{PT} + (\varepsilon_{PZT} - \varepsilon_{PT})V_{PT}} \quad (1)$$

where ε_{PT} and ε_{PZT} are dielectric constants of pure PT and pure PZT thin film; V_{PZT} and V_{PT} are the volume fractions of the PT and PZT materials in the multilayer films, respectively. For our film, V_{PZT} equals to $d_{PT}/(d_{PT} + d_{PZT})$ and V_{PT} equals to $d_{PT}/(d_{PT} + d_{PZT})$ as shown in Fig. 1. The equation provides a rough estimate of the dielectric constant of the multilayer films very roughly. The interfaces in the multilayer thin films that can cause film property deviation have been ignored. Moreover, the properties of PZT and PT layers within the multilayer thin films are different from that

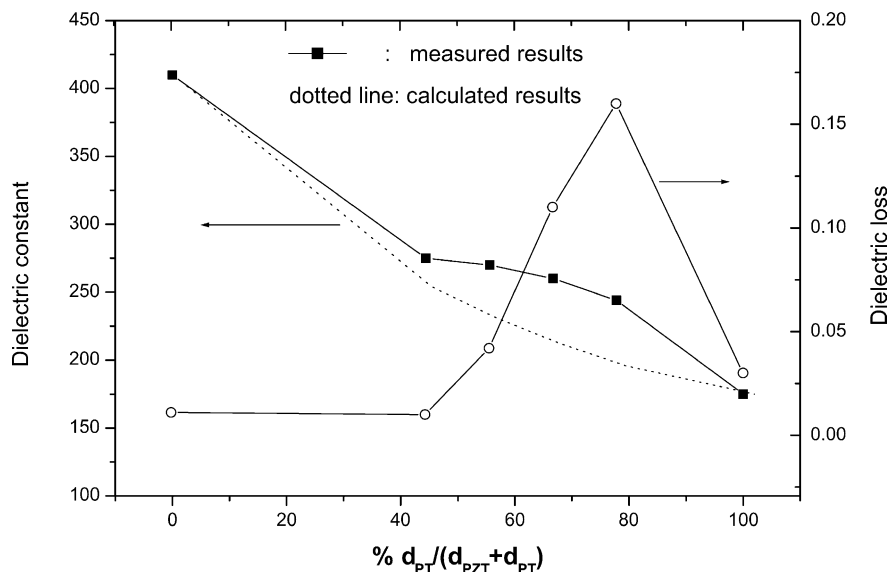


Fig. 5. Dielectric properties of the films as a function of PT volume fraction (30 Hz, 50 mV).

of the standalone ones, since they are deposited on different substrates. The pure standalone PZT and PT thin films are deposited on Pt substrate, while those PZT and PT layers inside the multilayer thin films are deposited either on PZT or PT layers. Fig. 5 shows the dielectric properties of the films as a function of the PT volume fraction measured at 30 Hz with an ac oscillation level of 50 mV. The dielectric constant of the multilayer thin films decreases when the PT volume fraction increases in the multilayer films due to the fact that the PT layer has much lower dielectric constant. Except for the sample 5PZT/4PT that has similar dielectric loss to those of pure PZT sample; all the other three types of multilayer samples exhibit much higher dielectric loss.

Sample 2PZT/7PT that has 350 nm PT inserted between two 50 nm PZT layers, has dielectric loss tangent of 0.173 at 30 Hz which are around 10 times of those of 5PZT/4PT and pure PZT thin films. More investigations will be done to understand the phenomenon.

3.3. Ferroelectric properties

Fig. 6a–e show the ferroelectric hysteresis loops of the pure PZT, 5PZT/4PT, 4PZT/5PT, 3PZT/6PT and 2PZT/7PT thin films, respectively. The pure PZT film shows normal hysteresis loop, however, all the other types of multilayer thin films have “pinched” or “double-loop-like” hystere-

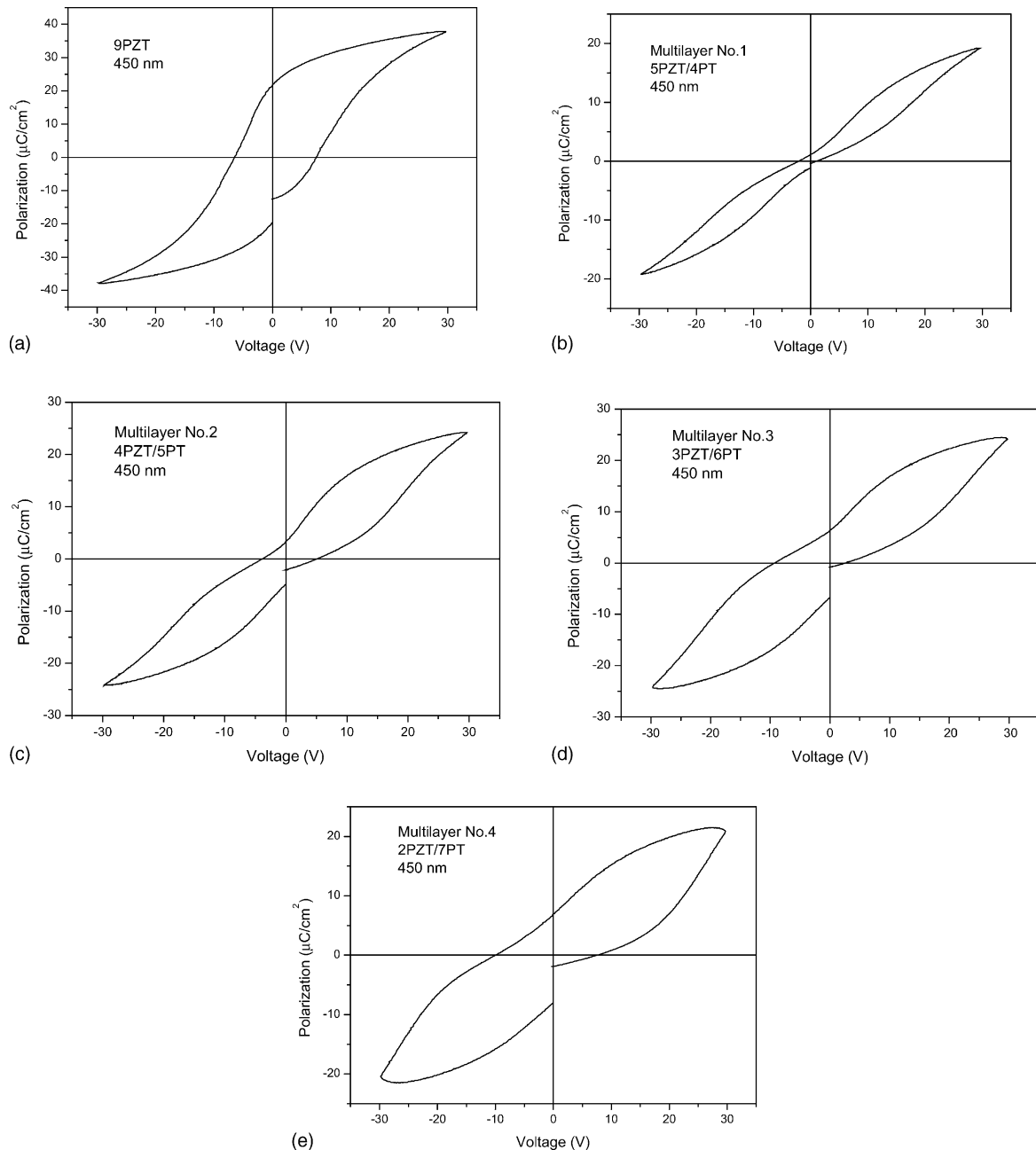


Fig. 6. *P*–*V* Hysteresis loops of (a) pure PZT; (b) 5PZT/4PT; (c) 4PZT/5PT; (d) 3PZT/4PT and (e) 2PZT/7PT.

sis loops. Multilayer films 4PZT/5PT, 3PZT/6PZT and 2PZT/7PT have “fatter” loops than film 5PZT/4PT due to their leaky property as shown in Fig. 4.

“Pinched” loops were observed after high-energy photo radiation to triglycine surface and PbTiO₃ single crystal [10,11], and were also reported in aged ferroelectric ceramics [12–16]. One suggested reason is the domain boundary pinning effects by defects or defects complexes. Defects or defects complexes can pin domain boundaries, preventing nucleation and growth of domains in the direction favored by an applied electrical field. At room temperature, lattice parameters for PbTiO₃ perovskite are $a = 3.916 \text{ \AA}$, $c = 4.157 \text{ \AA}$, and for PZT tetragonal perovskite, they are $a = 3.971 \text{ \AA}$, $c = 4.135 \text{ \AA}$ [17]. The lattice mismatch is defined as $(a_{\text{film}} - a_{\text{substrate}})/a_{\text{substrate}}$. Defects induced by lattice mismatch are expected to arise along the PZT and PT

interfaces. It may be the interface defects that act as domain pinning centers and cause the “pinched” hysteresis loops of the multilayer thin films. The “pinched” loops can be partially restored to the normal loops by ac-field cycling. During ac-field cycling, domain walls are repeatedly forced to move and thereby may become unpinned. This could be imagined as a multiple knocking of domain walls on defects or defect dipoles that leads to a redistribution of defects. Similar behavior has been observed by Jang and Yoon [18] in sol-gel derived Pb(Zr,Ti)O₃/PbZrO₃ multilayer thin films.

3.4. Pyroelectric property

The pyroelectric property of the 5PZT/4PT film is further investigated. The other three types of multilayer samples are rejected since they have high dielectric loss. The

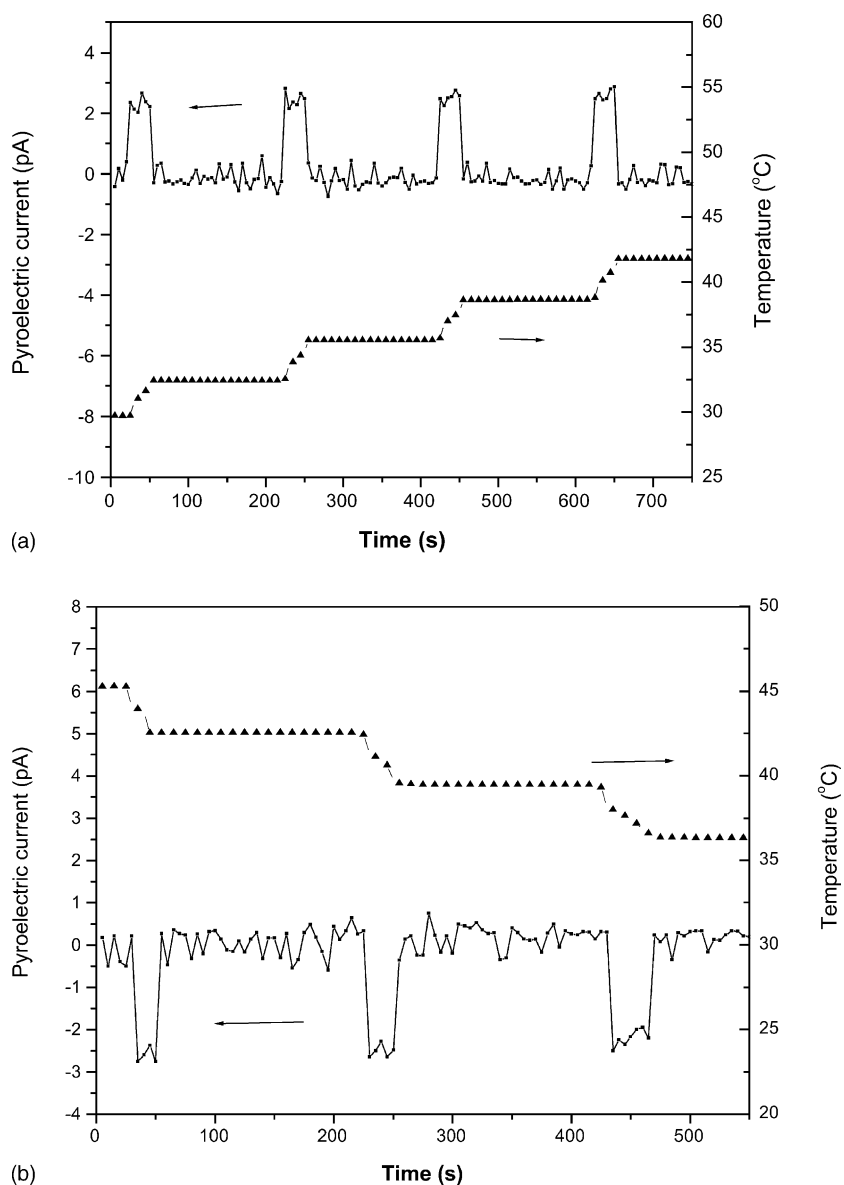


Fig. 7. Corresponding pyroelectric currents with a temperature (a) increasing rate and (b) decreasing rate of 6 °C/min.

Table 1
Properties comparison of multilayer 5PZT/4PT and pure PZT films

	Dielectric constant (30 Hz)		Dielectric loss tangent	Pyroelectric coefficient p ($\mu\text{C}/\text{m}^2 \text{ K}$)	F_D ($10^{-5} \text{ Pa}^{-1/2}$)
	Unpoled	Poled			
5PZT/4PT	273	204	0.014	250	2.1
PZT	410	318	0.013	290	1.7

pyroelectric coefficient of the sample is measured using the Byer–Roundy method. The sample is placed on a Linkam hot plate which is equipped with a temperature controller. The pyroelectric coefficient is measured by heating or cooling the sample and observing the induced pyroelectric current. Before pyroelectric coefficient measurement, the samples are poled. In order to optimize the pyroelectric property, the poling parameters have been systematically studied to find the best condition, which has been reported elsewhere [19]. The sample is poled at 350 kV/cm at 180 °C for 10 min. During pyroelectric coefficient measurement, the temperature of the sample is increased/decreased step by step as shown in Fig. 7. Fig. 7a shows a typical temperature profile with a step size of 6 °C/min and the corresponding pyroelectric current. The peaks correspond to the induced pyroelectric current while the steady-state current value is due to the background noise that comes from both the sample and the measurement system. The pyroelectric current induced by cooling the sample with the rate of 6 °C/min is shown in Fig. 7b. It is observed that the induced current with the same heating and cooling rates are symmetrical. The pyroelectric coefficient of the samples are calculated using the equation:

$$i_p = Ap' \frac{dT}{dt} \quad (2)$$

where i_p is the measured pyroelectric current, p' is the pyroelectric coefficient, A is the electrode area and dT/dt is the temperature change rate. The calculated pyroelectric coefficient of multilayer 5PZT/4PT is 250 $\mu\text{C}/\text{m}^2 \text{ K}$. Compared to the published results [20–22], the film shows good pyroelectric property.

For comparison, the pyroelectric property of pure PZT thin film is also characterized. Table 1 lists the properties of both films. The dielectric constant of the 5PZT/4PT multilayer film is lower than that of the pure PZT thin film, while their dielectric loss tangent are comparable. Although the pyroelectric coefficient of 5PZT/4PT multilayer film is measured to be slightly lower than that of the pure PZT film, the detectivity figure of merit is 23% better than that of pure PZT film due to the lower dielectric constant and similar dielectric loss tangent. The experiment results show that the 5PZT/4PT multilayer thin film is a better choice for developing high performance pyroelectric infrared detectors.

4. Conclusions

The properties of multilayer PZT/PT thin films with different PZT and PT layers stacking structures have been systematically studied. All the films are dense and smooth with single perovskite phase. The breakdown voltage of multilayer PZT/PT thin films are lower than those of pure PZT and PT thin films, since the applied voltage will mainly appear across on the PT layers that have lower dielectric constant and cause the PT layers to breakdown earlier. The dielectric constant of multilayer thin film decreases when the PT volume fraction increases because of much lower dielectric constant of PT. “Pinched” ferroelectric hysteresis loops are found for multilayer thin films. That may be caused by the defects induced domain pinning at the PZT and PT interfaces. After ac cycling, the “pinched” loops can be partially restored. The pyroelectric property of 5PZT/4PT thin film has been characterized. When compared to the pure PZT thin film, the 5PZT/4PT multilayer film has comparable pyroelectric coefficient, reduced dielectric constant and comparable dielectric loss. Therefore, the 5PZT/4PT thin film shows higher pyroelectric detectivity figure of merit and is promising for pyroelectric application.

References

- [1] S.R. Shannigrahi, H.M. Jang, Appl. Phys. Lett. 79 (2001) 1051.
- [2] M. Kohli, C. Wuethrich, K. Brooks, B. Willing, M. Forster, P. Muralt, N. Setter, P. Ryser, Sens. Actuators A 60 (1997) 147.
- [3] J.F. Roeder, I.S. Chen, P.C. Van Buskirk, H.R. Beratan, C.M. Hanson, Proceedings of the Eleventh IEEE International Symposium on Application of Ferroelectrics, vol. 217, 1998.
- [4] R.E. Newnham, G.R. Ruschau, J. Am. Ceram. Soc. 74 (1991) 463.
- [5] K. Aoki, Y. Fukuda, K. Numata, A. Nishimura, Jpn. J. Appl. Phys. 35 (1996) 2210.
- [6] I. Kanno, S. Hayashi, T. Kameda, M. Kitakawa, T. Hirao, Jpn. J. Appl. Phys. 32 (1993) 4057.
- [7] Y. Ohya, T. Ito, Y. Takahashi, Jpn. J. Appl. Phys. 33 (1994) 5272.
- [8] W.G. Liu, W.G. Zhu, O.K. Tan, Proceedings of the First International Conference on Thermophysical Properties of Materials, Singapore, 1999.
- [9] J.J. Shyu, P.C. Lee, Jpn. J. Appl. Phys. 35 (1996) 3954.
- [10] G.H. Jonker, J. Am. Ceram. Soc. 55 (1972) 57–58.
- [11] R.C. Bradt, G.S. Ansell, J. Am. Ceram. Soc. 52 (1969) 192–199.
- [12] H. Dederichs, G. Arlt, Ferroelectrics 68 (1986) 281–292.
- [13] K. Carl, K.H. Härdtl, Ferroelectrics 17 (1978) 473–486.
- [14] B. Jaffe, W.R. Cook Jr., H. Jaffe, Piezoelectric Ceramics, Academic, Marietta, OH, 1971.

- [15] M.E. Lines, A.M. Glass, Principles and Applications of Ferroelectrics and Related Materials, Clarendon, Oxford, 1977.
- [16] D. Lupascu, V. Shur, A. Shur, Appl. Phys. Lett. 80 (2002) 2359.
- [17] C.H. Park, D.J. Chadi, Phys. Rev. B 57 (1998) R13961.
- [18] J.H. Jang, K.H. Yoon, Appl. Phys. Lett. 75 (1) (1999) 130.
- [19] L.L. Sun, O.K. Tan, W.G. Liu, W.G. Zhu, X. Yao, Infrared Phys. Tech. 44 (3) (2003) 177.
- [20] A. Bell, Y. Huang, O. Paul, Y. Nemirovsky, N. Setter, Integr. Ferroelectrics 6 (1995) 231.
- [21] M. Kohli, C. Wuthrich, K. G Brooks, B. Willing, M. Forster, P. Muralt, N. Setter, P. Pyster, Sens. Actuators A 60 (1997) 147.
- [22] N.M. Shorrocks, A. Patel, M.J. Walker, A.D. Parsons, Microelectron. Eng. 29 (1995) 59.